Highly regenerative species-specific genes improve age-associated features in the adult *Drosophila* midgut

Hiroki Nagai[1,3], Yuya Adachi[1], Tenki Nakasugi[1], Ema Takigawa[1], Junichiro Ui[1], Takashi Makino[2], Masayuki Miura[1] and Yu-ichiro Nakajima[1*]

Abstract

Background The remarkable regenerative abilities observed in planarians and cnidarians are closely linked to the active proliferation of adult stem cells and the precise differentiation of their progeny, both of which typically deteriorate during aging in low regenerative animals. While regeneration-specific genes conserved in highly regenerative organisms may confer regenerative abilities and long-term maintenance of tissue homeostasis, it remains unclear whether introducing these regenerative genes into low regenerative animals can improve their regeneration and aging processes.

Results Here, we ectopically express highly regenerative species-specific JmjC domain-encoding genes (HRJDs) in *Drosophila*, a widely used low regenerative model organism. Surprisingly, HRJD expression impedes tissue regeneration in the developing wing disc but extends organismal lifespan when expressed in the intestinal stem cell lineages of the adult midgut under non-regenerative conditions. Notably, HRJDs enhance the proliferative activity of intestinal stem cells while maintaining their differentiation fidelity, ameliorating age-related decline in gut barrier functions.

Conclusions These findings together suggest that the introduction of highly regenerative species-specific genes can improve stem cell functions and promote a healthy lifespan when expressed in aging animals.

Keywords Synthetic biology, Aging, Healthy lifespan, Regeneration, *Drosophila*, Intestinal stem cells

Background

Regeneration, an intricate process that rebuilds lost body parts, is a widespread phenomenon among metazoans, but the capacity for regeneration displays significant variation across different groups and species [1–5].

While certain animals like planarians and hydras possess the remarkable ability to regenerate their entire body from a small fragment, other groups with more complex body structures, such as mammals and insects, exhibit a diminished regenerative potential and can only regenerate specific tissues and/or organs to a limited extent. Furthermore, regenerative capacity often declines with aging in most species with limited regeneration abilities [2], resulting in increased susceptibility to organismal death upon injury. In contrast, animals that can achieve whole body regeneration, along with developmental reversion observed in the jellyfish *Turritopsis*, exhibit potential immortality [2, 5, 6]. Understanding the mechanisms underlying high regenerative ability and their relationship with aging represents a fundamental challenge in

*Correspondence:
Yu-ichiro Nakajima
nakaji97@g.ecc.u-tokyo.ac.jp
[1] Graduate School of Pharmaceutical Sciences, The University of Tokyo, 7-3-1 Hongo, Bunkyo-Ku, Tokyo 113-0033, Japan
[2] Graduate School of Life Sciences, Tohoku University, 6-3 Aramaki Aza Aoba, Aoba-Ku, Sendai 980-8578, Japan
[3] Institute of Science and Technology Austria, Am Campus 1, 3400 Klosterneuburg, Austria

Nagai *et al. BMC Biology* (2024) 22:157

Page 2 of 16

the field of developmental biology and gerontology with implications for regenerative medicine.

Several cellular and molecular factors have been identified as determinants of regeneration capacity. Highly regenerative animals such as planarians and cnidarian polyps rely on pluripotent adult stem cells, called neoblasts and interstitial cells (i-cells), respectively [2–5, 7]. These stem cells migrate to the injury sites and contribute to the formation of a blastema, an undifferentiated cellular mass, enabling the restoration of amputated body structures. Some vertebrates like salamanders and fish, which do not possess adult pluripotent stem cells, can regenerate organs after injury by recruiting blastema cells through dedifferentiation and/or the activation of quiescent lineage-restricted stem cells [1, 2, 4, 5, 8]. At the molecular level, the evolutionary conserved WNT signaling pathway promotes a wide range of regenerative events across species, including blastema formation in newts and *Hydra* [1–5, 8].

In contrast to the conserved regulators of regeneration, several genes are specific to highly regenerative animal groups and species: for instance, the newt gene *Prod1* regulates re-patterning during limb regeneration [9, 10], and viropana family (*viropana 1–5*) is upregulated during lens regeneration [11, 12]. These species/group-specific genes might explain differences in regeneration capacity between species. Remarkably, ectopic expression of *viropana 1–5* can enhance regeneration of the primordium of *Drosophila* eyes that maintain regenerative capacity during development [12]. This finding raises the possibility that heterologous induction of regenerative genes may accelerate tissue regeneration, at least in developing animals, and potentially provide a cue for developing novel regenerative therapies. However, it remains unknown whether heterologously-induced regenerative genes can improve regenerative and/or aging processes even when induced in post-developmental mature adults.

Notably, given that basal metazoans such as Porifera, Ctenophore, Placozoa, and Cnidaria all exhibit robust regenerative abilities, it is conceivable that a common ancestor of all metazoans once possessed a high regenerative potential and independently lost genes related to high regenerative capacity in multiple phyla. Building upon this hypothesis, bioinformatics analysis has identified genes that are common among species with high regenerative abilities and absent in species with limited regenerative capacities (Fig. 1A) [13]. The *h*ighly *r*egenerative species-specific *J*mjC *d*omain-encoding genes (HRJDs) are a group of such genes (with typically two or three orthologs per species) characterized by their JmjC domain (Fig. 1A), yet their molecular functions remain unknown. Given their potential influence on the regenerative process, HRJDs may contribute to the high

regeneration potential of highly regenerative animals. With this in mind, a question arises: what would happen if a low regenerative species, which has lost HRJDs, were to acquire them again? By ectopically expressing HRJDs in low regenerative animal models, we can investigate their impacts on regeneration as well as on aging processes, providing insight into the role of HRJDs.

Here, we express HRJDs in the fruit fly *Drosophila melanogaster* and evaluate their impact in vivo, especially by focusing on two epithelial tissues: developing wing discs and post-developmental adult midguts, both of which exhibit regeneration potential and can replenish damaged epithelial cells. In contrast to the predicted contribution of HRJDs in regeneration as observed in planarian, ectopic HRJD induction impedes regenerative responses and decreases organismal survival upon injury in *Drosophila*. Surprisingly, however, HRJD expression in the stem/progenitor population of the adult midguts extends organismal lifespan under the non-regenerative condition. Further investigations reveal that HRJDs enhance the proliferative activity of intestinal stem cells while keeping their differentiation fidelity in aged guts, ameliorating age-related decline in gut barrier functions. These findings provide evidence that genes specific to highly-regenerative animals can improve stem cell function as well as increase healthy lifespan upon heterologous expression in aging animals.

Results

Planarian HRJD expression does not affect gross morphology of fly adults

Planarians are one of the most highly regenerative animals; they are capable of regenerating most body parts upon amputation and can even reconstruct their whole body from fragments [1–4, 8, 14]. Previous work has identified two HRJD orthologs *HRJDa* and *HRJDb* from two planarian species, *Dugesia japonica* and *Schmidtea mediterranea*, where both HRJDs contain only the JmjC domain and the EF hand motif (Fig. 1B) [13]. In functional assays using RNAi-mediated knockdown in *D. japonica*, these two HRJDs affect viability of organisms after amputation [13], suggesting that planarian HRJDs are associated with regeneration processes. We thus utilized these functional HRJDs in *D. japonica* as representatives for the following studies and hereafter simply named them as HRJDa and HRJDb.

To examine potential benefits and/or disadvantages of acquiring HRJDs, we then ectopically expressed HRJDs in *Drosophila melanogaster*, which has lost HRJD genes during evolution (Fig. 1A), using the Gal4/UAS system (Additional file 1: Fig. S1) [15]. We first introduced HRJDs in the whole body throughout development with the ubiquitous driver *Act5C-Gal4* (Fig. 1C,
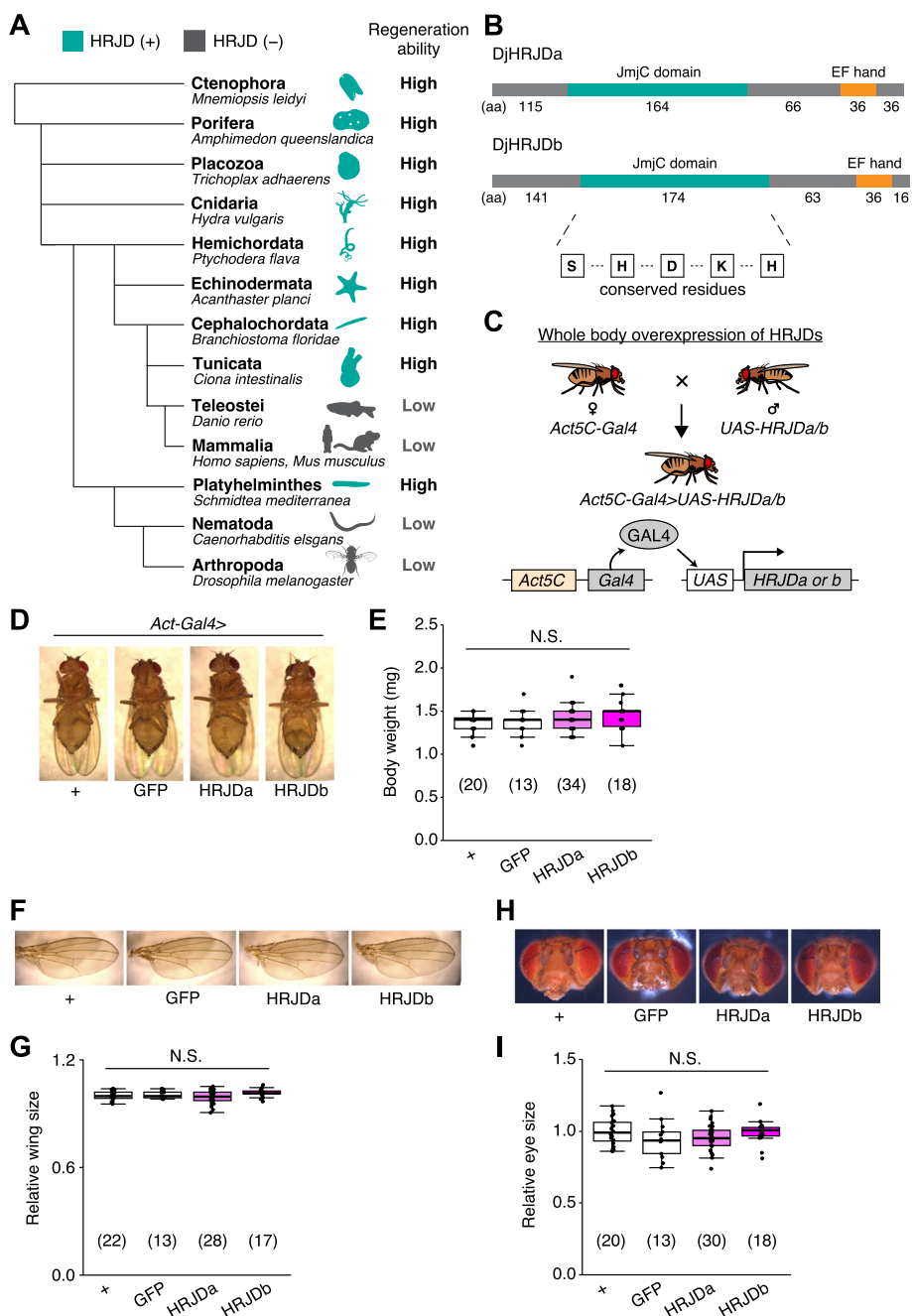
Nagai *et al. BMC Biology* (2024) 22:157

Page 3 of 16

Fig. 1 HRJD expression in whole body does not affect gross morphology. **A** Phylogenetic tree of HRJD conservation. Green indicates species that possess HRJD gene(s) and gray indicates species that have lost HRJD gene(s). High regenerative ability indicates that the species can regenerate their whole body or anterior/posterior body parts, and low regenerative ability indicates that the species can only regenerate their appendage (limbs, tails, fins) or much smaller scale of tissues/organs. We referred to Cao et al. (2019) for the definition of regenerative ability [13]. **B** Protein sequence of HRJDs used in this study, which derived from *Dugesia japonica* (DjHRJDa/b, hereafter simply described as HRJDa/b). Conserved residues characteristic of the JmjC domain are shown. **C** Schematics of genetic experiments for whole body induction of HRJDs. The Gal4-UAS system enables gene expression downstream of the UAS sequence, which is regulated by the transcription factor Gal4 [15]. In this case, the ubiquitously active *Act5C* promoter is used for Gal4 expression. **D** Representative images of mature adults for whole body expression of HRJDs. **E** Whole body induction of HRJDs did not change body weight of mature adults. **F** Representative images of adult wings. **G** Whole body induction of HRJDs did not change wing size. **H** Representative images for adult heads. **I** Whole body induction of HRJDs did not change eye size of adult flies. N.S., not significant: $P > 0.05$. One-way ANOVAs with post hoc Tukey test. *n* indicates the number of flies examined. See also Additional file 1: Fig. S1

Nagai *et al. BMC Biology* (2024) 22:157

Page 4 of 16

Act5C-Gal4 > UAS-HRJDa/b). The whole body expression of HRJDs neither caused developmental lethality nor changed the body weight of mature adults compared with the *Act5C-Gal4 > UAS-GFP* control (Fig. 1D, E). We further assessed the gross morphology of adult wings and eyes under the ubiquitous expression of HRJDs. The wing size was not altered by HRJD expression (Fig. 1F, G). Similarly, *Act5C-Gal4 > UAS-HRJDa/b* flies did not change the size of adult compound eyes (Fig. 1H, I). These results indicate that HRJD expression does not disturb gross morphology of adult flies under homeostatic conditions, likely due to minimal impacts on developmental processes.

HRJD expression hampers tissue regeneration in the developing wing disc

Given that HRJDs are conserved only among highly regenerative animals, their primary functions may be related to regeneration processes. Indeed, both planarian HRJDa and HRJDb function in whole-body regeneration while their relative contribution is likely context-dependent: HRJDa is indispensable for the regeneration of amputated heads while HRJDb promotes organismal survival after two consecutive amputations [13]. To test whether heterologously-induced HRJDs can enhance regenerative responses in *Drosophila*, we examined their impacts on regeneration after ablation of the developing wing imaginal disc. The *Drosophila* larval imaginal discs, including wing discs, which are composed of columnar epithelial cells, exhibit regenerative capacity and restore morphology even after massive cell death [16, 17] (Fig. 2A, B). We utilized the genetic ablation system in which transient overexpression of *eiger*, a *Drosophila* TNF ligand, induces apoptosis in the wing pouch region [17, 18]. In this tissue ablation system, the temperature-sensitive form of the Gal4 repressor Gal80 (*tub-Gal80^ts*) allows transient tissue ablation under the control of a wing pouch driver *rn-Gal4*. To circumvent the temporal expression associated with the Gal4/Gal80^ts system, we further introduced an additional binary expression system: the QF/QUAS system for HRJD induction (Fig. 2A) [19, 20]. When expressing HRJDs in the wing pouch with the *WP-QF2* driver during the entire process of recovery, we found that *WP-QF2 > QUAS-HRJDs* flies exhibit severe defects compared to controls (Fig. 2C). Immunostaining of a mitotic marker, phosphohistone H3 (PH3), revealed that HRJD expression did not cause statistically significant difference in regenerative proliferation in the wing pouch (Fig. 2D, E). Nevertheless, it is possible that insufficient damaged cell replenishment may occur in these conditions. Importantly, HRJD induction in the wing disc affected neither the development of the adult wing nor proliferation in wing discs under homeostatic condition

(Fig. 2F–I). These results suggest that HRJD expression does not facilitate regeneration in the developing wing disc epithelium.

HRJD expression compromises regeneration in the adult midgut

Most highly regenerative animals exhibit regeneration potential in mature adult stages [2–4, 8], and thus one possibility is that HRJDs stimulate regenerative responses only in adults, where tissue-resident stem cells play an important role in homeostasis and regeneration. We thus tested the impact of HRJD expression on the regenerative capacity of the *Drosophila* adult midgut. In the adult midgut, intestinal stem cells (ISCs) self-renew ISCs themselves and also generate differentiating progenitor cells called enteroblasts (EBs) and enteroendocrine progenitors (EEPs), which eventually differentiate into absorptive enterocytes (ECs) and secretory enteroendocrine cells (EEs), respectively (Fig. 3A) [21–24]. The adult midgut activates proliferation of ISCs in response to orally-treated harmful chemicals such as paraquat and dextran sulfate sodium (DSS), a regenerative response that is essential for organismal survival [21, 25–28]. We thus expressed HRJDs in ISCs and EBs using the *esg-Gal4* (*esg-Gal4 > UAS-HRJDa/b*) driver and tested survival against paraquat/DSS damage. Similar to the wing regeneration assay, continuous expression of HRJDs via *esg-Gal4* significantly impaired organismal survival upon the chemical challenges, with a stronger effect for HRJDa (Additional file 1: Fig. S2A and S2B). By contrast, survival during 11 days of control feeding (5% sucrose) was not significantly decreased by HRJD expression (Additional file 1: Fig. S2C), raising a possibility that abnormal regenerative response compromises the survival upon intestinal damage. We thus examined ISC proliferation after paraquat feeding by counting the number of cells marked with a mitotic marker, anti-PH3 staining, and found that induction of HRJDa significantly suppressed ISC division (Additional file 1: Fig. S2D), which is consistent with the stronger decline in survival rate. Concordant with the wing ablation experiments, these results suggest that continuous HRJD expression causes detrimental effects to regenerative capacity.

Because the *esg-Gal4* driver is active not only in adult ISCs/EBs but also in the proliferative adult midgut progenitors in the larval midguts and larval imaginal discs [29, 30], continuous HRJD expression may cause internal organ defects associated with development. To temporally restrict HRJD expression to the adult stage, we next set up an experiment where HRJD expression starts only in adults after eclosion from pupa by combining *esg-Gal4* with *tub-Gal80^ts* (*esg-Gal4^ts > UAS-HRJDa/b*) (Fig. 3B); however, neither HRJDa nor

Nagai *et al. BMC Biology* (2024) 22:157
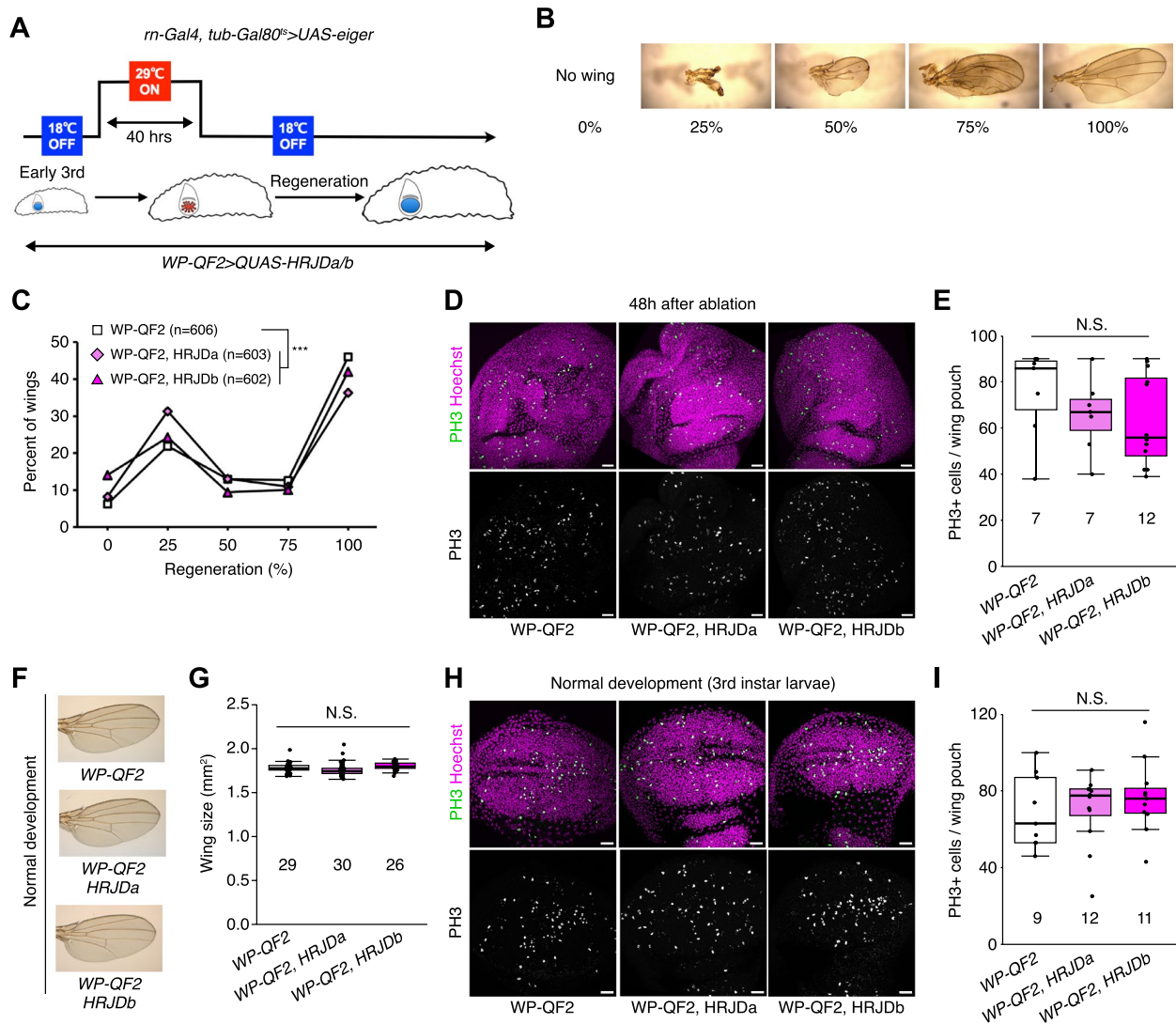
Page 5 of 16

Fig. 2 HRJD expression impedes tissue regeneration in the developing wind disc. **A** Schematics of genetic ablation of the wing disc. TNF ligand *eiger* was overexpressed in the wing pouch for 40 h during the larval stage. **B** Wing regeneration was assessed in the adult stage by checking the size of wing (0%: no wing, 100%: intact wing). **C** Line graph for wing regeneration. Expression of HRJDa/b increased the rate of low regeneration (0% and 25%) at the expense of the rate of full regeneration (100%). **D**, **E** Representative images for PH3 staining of wing discs during regeneration at 48 h after ablation (**D**). The number of PH3 positive cells is quantified in **E**. **F**, **G** Representative images for adult wings of *WP-QF2 > QUAS-HRJDa/b* flies under homeostatic (non-regenerative) condition (**F**). The wing size is quantified in **G**. **H**, **I** Representative images for PH3 staining of wing discs (3rd instar larvae) during normal development (**H**). The number of PH3 positive cells is quantified in **I**. N.S., not significant: $P > 0.05$, ***$P \leq 0.001$. Chi-square test (**C**) and one-way ANOVAs with post hoc Tukey test (**E**, **G**, **I**). *n* indicates the number of wings (**C**, **G**) and wing discs (**E**, **I**) examined. Scale bars: 20 µm

HRJDb improved organismal survival upon paraquat/DSS feeding (Fig. 3C, D). Instead, HRJDa expression caused a slight but significant decrease in survival rate compared to controls (*esg-Gal4^{ts} > UAS-GFP*), while HRJDb expression did not lead to a statistically significant decline of survival (Fig. 3C, D). Survival under control feeding (5% sucrose) was comparable between *esg-Gal4^{ts} > UAS-GFP* and *esg-Gal4^{ts} > UAS-HRJDa/b*

(Fig. 3E), suggesting that the impaired survival of *esg-Gal4^{ts} > UAS-HRJDa* is specific to regenerative contexts. We also found that, after paraquat feeding, mitotic cell numbers in HRJD expressing flies decreased slightly (Fig. 3F, G), suggesting the possibility of impaired regeneration. These results indicate that post-developmental expression of HRJDs does not enhance intestinal regeneration in adult flies.
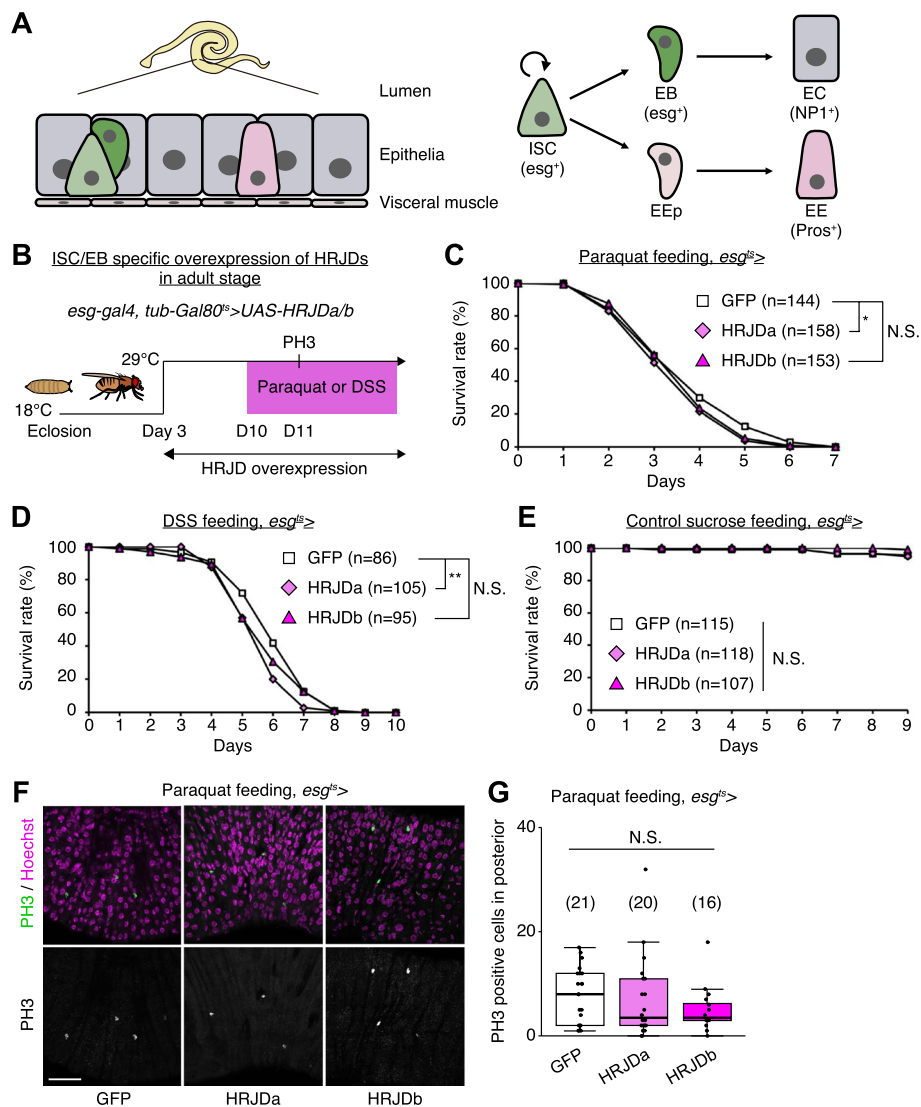
Nagai *et al. BMC Biology* (2024) 22:157

Page 6 of 16

Fig. 3 HRJD expression compromises regeneration in the adult midgut. **A** Schematics of the *Drosophila* adult midgut. The adult midgut is a pseudostratified epithelium, in which intestinal stem cells (ISCs) generate both absorptive enterocytes (ECs) and secretory enteroendocrine cells (EEs) through progenitor cell enteroblasts (EBs) and EE progenitor cells (EEPs). **B** Experimental scheme for ISC/EB specific induction of HRJDs under the *esg-Gal4* driver in the adult stage. Adult flies were transferred to 29 °C at day 3 to induce HRJD expression. **C–E** Survival curve during paraquat (**C**), DSS (**D**), and sucrose (**E**) feeding. **F** Representative images for PH3 staining upon paraquat feeding. **G** Quantification of PH3 positive cells in posterior midguts. N.S., not significant: $P > 0.05$, *$P < 0.05$, **$P \leq 0.01$. Log-rank test. *n* indicates the number of flies (**C–E**) and midguts (**G**). Scale bars: 50 µm. See also Additional file 1: Fig. S2

Post-developmental HRJD expression in ISC lineages extends organismal lifespan

Highly-regenerative animals are often resistant to organismal aging and have long lifespan; some species like the jellyfish *Turritopsis* even revert their early developmental stages under harsh environments and are considered to be potentially immortal [2, 6]. Although heterologous expression of HRJDs does not augment tissue regeneration in either developing or adult *Drosophila* tissues, we further investigated whether HRJDs influence organismal lifespan under homeostatic conditions in which no experimental injuries are applied to fly adults. We observed that post-developmental HRJD expression in adult ISCs/EBs (*esg-Gal4ts > UAS-HRJDa/b*) significantly extended organismal lifespan both in females (Fig. 4A) and males (Fig. 4B). In contrast, continuous HRJD expression in the whole body (*Act5C-Gal4 > UAS-HRJDa/b*) shortened males' lifespan (Fig. 4C, D). Moreover, HRJD expression in differentiated ECs (*NP1-Gal4 > UAS-HRJDa/b*) also negatively impacted female lifespan, likely due to
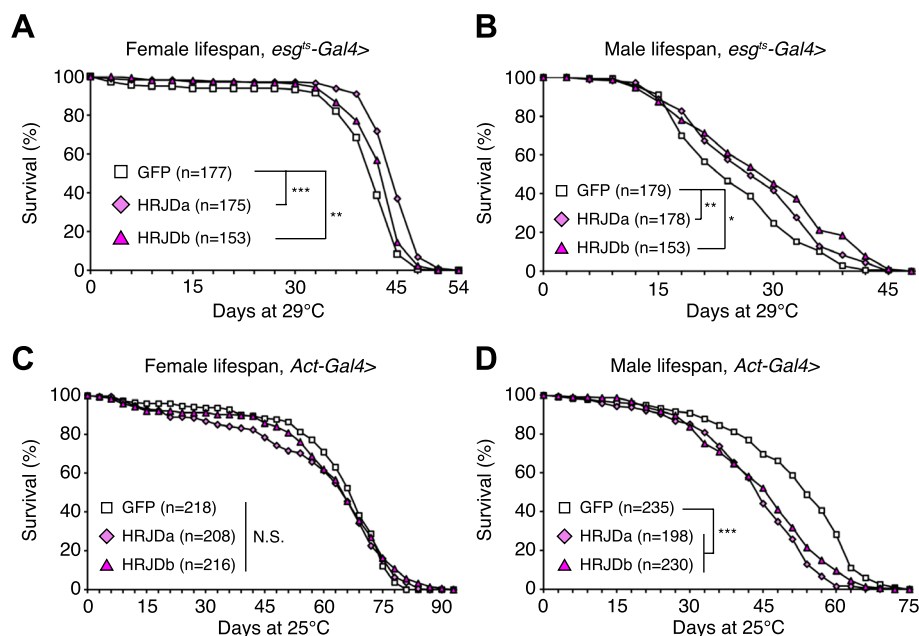
Nagai *et al. BMC Biology* (2024) 22:157

Page 7 of 16

Fig. 4 Post-developmental HRJD expression in ISC lineages extends organismal lifespan. **A**–**D** Survival curve for organismal lifespan by sex. HRJDs are induced by *esg^{ts}-Gal4* (**A** and **B**) and *Act5C-Gal4* (**C** and **D**). For temporal regulation of HRJD induction using *tub-Gal80^{ts}* (**A** and **B**), adult flies were transferred to 29 ℃ at day 3. N.S., not significant: $P > 0.05$, *$P < 0.05$, **$P \leq 0.01$, ***$P \leq 0.001$, Log-rank tests. *n* indicates the number of flies. See also Additional file 1: Fig. S3

developmental abnormalities since EC-specific HRJD expression in the adult stage did not decrease survival (Additional file 1: Fig. S3A-S3D). These results suggest that spatio-temporally regulated induction of HRJDs in adult ISCs/EBs can be beneficial for adult flies under homeostatic conditions.

Further investigation revealed the distinct impacts of HRJDa and HRJDb on organismal lifespan: while continuous expression of HRJDa via *esg-Gal4 (esg-Gal4 > UAS-HRJDa)* shortened lifespans for both males and females, *esg-Gal4 > UAS-HRJDb* prolonged female lifespans but shortened male lifespans (Additional file 1: Fig. S3E and S3F). The ortholog-dependent phenotypic differences were also reported in planarian regeneration [13]. To address the mechanisms of lifespan extension associated with post-developmental HRJD expression in ISCs/EBs, we focused on *esg-Gal4^{ts} > UAS-HRJDs* midguts in the following experiments.

HRJD expression improves barrier function in the aged intestine

Age-related mortality accompanies intestinal barrier dysfunction and disruption of cell–cell junction in the gut epithelium across species [31–34]. Given that aging phenotypes are more severe in female flies than male flies [35], we first tested barrier function of the *esg-Gal4^{ts} > UAS-HRJDa/b* female midgut using the Smurf

assay, in which orally-administered blue dye spreads throughout the entire body when the intestinal barrier is disrupted (Smurf+, Fig. 5A) [31, 35]. Consistent with lifespan extension, post-developmental HRJD expression in ISCs/EBs significantly decreased the ratio of Smurf+ adults at 30 days old, a time point where age-related organismal death starts (Fig. 4A and Fig. 5A), suggesting that barrier function is maintained in aged flies that express HRJDs in ISCs/EBs. We further assessed the localization of septate junction markers (Dlg, Tsp2A, Mesh, Ssk), which diffuse in cytoplasm in the aged midgut [33, 36–38]. The diffusion of the Dlg protein in aged midguts was significantly suppressed in *esg-Gal4^{ts} > UAS-HRJDa/b* midguts (Fig. 5B, C). Similarly, peripheral localization of Tsp2A, Mesh, and Ssk proteins was also maintained in *esg-Gal4^{ts} > UAS-HRJDa/b* midguts compared with control (*esg-Gal4^{ts} > UAS-GFP*) midguts (Fig. 5D–I). Given that HRJDs in ISCs/EBs affect localization of junctional components in ECs, we next tested if HRJDs non-autonomously affect junctional integrity. To this end, we performed a mosaic experiment where HRJDs were clonally induced using the esgFLPout system [26]. Clonal induction of HRJDs improved junctional localization of Ssk both inside and outside the clones (Additional file 1: Fig. S4A and S4B), supporting the conclusion that HRJDs' effect is non-cell autonomous. We then examined JNK activation in ECs, which is associated
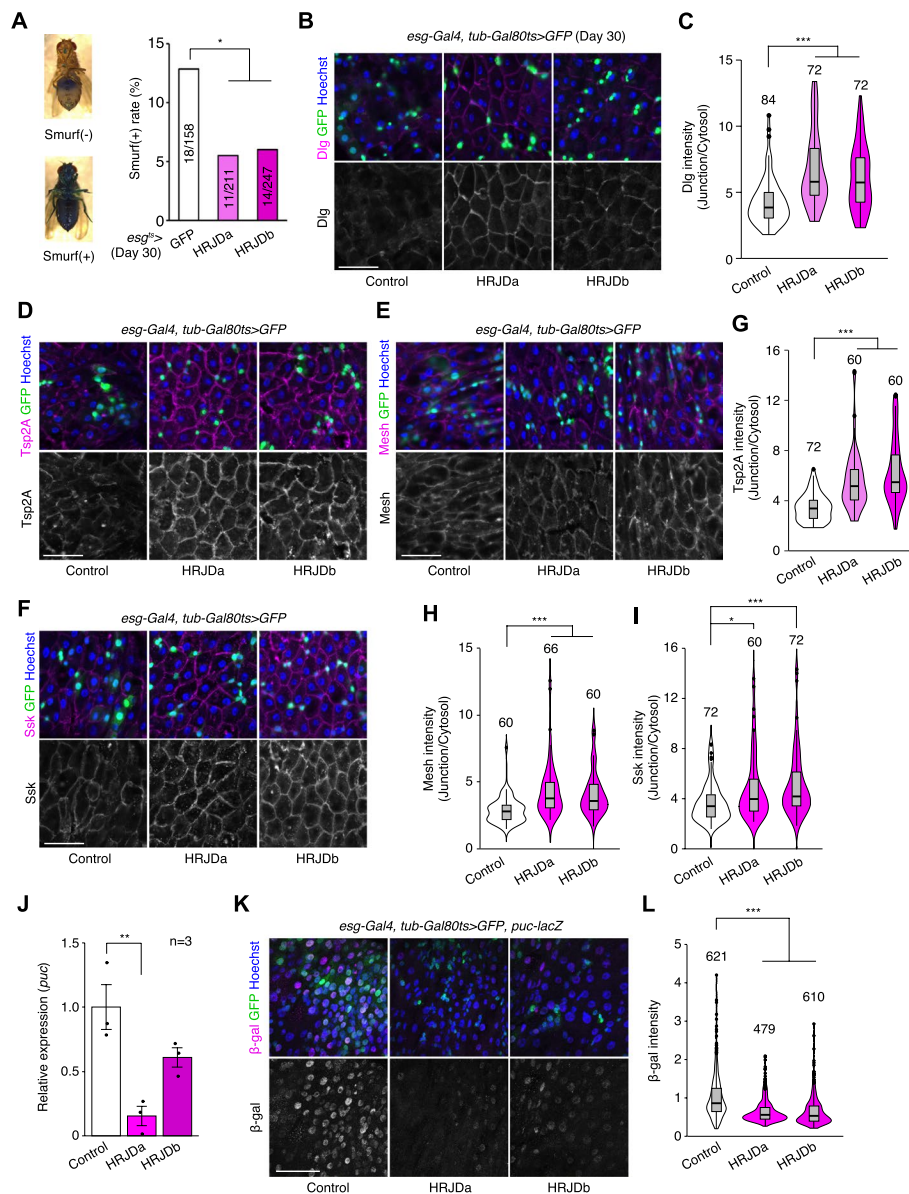
Nagai *et al. BMC Biology* (2024) 22:157

Page 8 of 16

Fig. 5 HRJD expression in adult ISCs/EBs suppresses age-related gut barrier dysfunction. **A** *esg^ts*-mediated HRJD induction decreased Smurf(+) ratio at day 30. The representative images of the Smurf phenotype (leakage of blue dye throughout whole body) are shown on the left. **B, C** HRJD expression in adult ISCs/EBs maintained junctional localization of Dlg protein in ECs, which is quantified in **C**. **D–I** HRJD expression in adult ISCs/EBs maintained junctional localization of Tsp2A (**D**), Mesh (**E**), and Ssk (**F**) in ECs, which is quantified in **G–I**. **J** RT-qPCR of *puc* in the whole midgut. *esg^ts*-mediated induction of HRJDa significantly repressed *puc*. **K, L** *puc-lacZ* intensity in polyploid cells was decreased by HRJD expression (**K**), which is quantified in (**L**). *$P < 0.05$, **$P < 0.01$, ***$P \leq 0.001$, one-way ANOVAs with post hoc Tukey test. *n* indicates the number of flies (**A**), cells (**C, G, H, I, L**), and biological replicates (**J**). Scale bars: 50 μm

with barrier dysfunction in the aged intestine [27, 36]. HRJD expression in ISCs/EBs significantly repressed transcription of *puckered* (*puc*), a downstream target of JNK signaling in the whole midgut (Fig. 5J)), and indeed the intensity of *puc-lacZ* reporter decreased in ECs upon HRJD induction (Fig. 5K, L). HRJD expression in ISCs/

EBs thus suppresses JNK signaling in ECs in the aged midgut, which is mediated by either a non-autonomous function of HRJDs or residual HRJD proteins in newly differentiated ECs. These results indicate that HRJD expression in adult ISCs/EBs contributes to the prolonged maintenance of the junctional integrity as well as gut barrier function in the aged intestine.

HRJD expression attenuates mis-differentiation of stem cell lineage in the aged intestine

In addition to the intestinal barrier dysfunction, aberrant activation of ISC mitosis and accumulation of mis-differentiated ISC progenies are also common age-related phenotypes in the *Drosophila* adult midgut [27, 31, 33, 39]. In 30-days old control midguts, *esg-Gal4^{ts} > UAS-GFP$^+$* cells exhibited hallmarks of age-related mis-differentiation into ECs such as increased ploidy and enlarged nuclear size (Fig. 6A) [27]. By contrast, we found that HRJD expression in adult ISCs/EBs suppressed these mis-differentiation phenotypes (Fig. 6A, B), which are consistent with the amelioration of age-related barrier dysfunction in *esg-Gal4^{ts} > UAS-HRJDa/b* midguts. Surprisingly, however, *esg-Gal4^{ts} > UAS-HRJDa/b* did not suppress age-related increase in ISC proliferation but rather enhanced it in 30-day old midguts (Fig. 6C, D). The enhancement of ISC proliferation was specific to the aged intestine since *esg-Gal4^{ts} > UAS-HRJDs* did not affect PH3$^+$ cell number in 10-day-old young midguts (Additional file 1: Fig. S4E). These results raised the possibility that HRJD expression augments the mitotic activity of stem cells while maintaining their differentiation fidelity during aging.

To test this hypothesis, we first measured the expression of cell type markers (*Delta* for ISCs, *nub* for ECs, and *pros* for EEs) by RT-qPCR of whole midguts. Both *nub* and *pros* are negatively regulated by Esg [40, 41], and accumulation of *esg$^+$* mis-differentiated cells accompanies the downregulation of EC-related genes in aged midguts [27]. Consistent with enhanced ISC proliferation, *esg-Gal4^{ts} > UAS-HRJDa* significantly upregulated *Delta* (*Dl*) expression in 30-day old midguts (Fig. 6E). More importantly, *esg-Gal4^{ts} > UAS-HRJDa* also upregulated *nub* and *pros*, which supports our hypothesis that HRJDs improve proper differentiation of ISC progenies. In *esg-Gal4^{ts} > UAS-HRJDb*, only *Dl*, but not *nub* and *pros*, was upregulated when whole midguts were used as sample (Fig. 6E). Next, we focused on the posterior midgut where both HRJDa and HRJDb prevent mis-differentiation of EBs (Fig. 6A) and examined cell type composition using the combination of markers *esg^{ts} > GFP* (ISC/EB), *Dl-lacZ* (ISC/EEP), and anti-Pros (EEP/EE). Consistent with the prevention of EB mis-differentiation, *esg^{ts}*-mediated HRJD expression decreased EBs (esg$^+$Dl$^-$Pros$^-$) and increased polyploid ECs (esg$^-$Dl$^-$Pros$^-$) compared to the control midgut (Fig. 6F, G). These results indicate that HRJDs improve differentiation fidelity in ISC lineage.

To address the potential mechanism of HRJD-dependent maintenance of ISC functions, we focused on the JAK-STAT pathway since its activation promotes both ISC proliferation and differentiation into ECs [26, 42, 43]. In young mature midguts, STAT activity is largely restricted to *esg$^+$* ISCs/EBs [26, 42, 44]. In aged midguts,

however, a subset of polyploid cells exhibited weak signal of the STAT reporter *10×STAT-GFP*, likely due to the accumulation of mis-differentiated EBs (Fig. 6H). Notably, HRJD induction canceled such ectopic STAT activation in polyploid cells and rather enhanced STAT activity in diploid ISCs/EBs (Fig. 6H, I), which is consistent with our observations that HRJDs boost ISC functions during aging. These results suggest that HRJD expression accelerates the generation of differentiated ECs via JAK-STAT activation. In the healthy homeostatic intestine, ISC division and subsequent differentiation into ECs is coupled with the loss of old ECs [45, 46]. Interestingly, we found that *esg*-lineage clones that express HRJDs rapidly replaced pre-existing cells by generating polyploid ECs (Additional file 1: Fig. S4A, S4C, and S4D). In addition, more cells exhibited cleaved Dcp1, an apoptotic marker [47, 48], in 30-day old *esg^{ts} > HRJDs* midguts (Additional file 1: Fig. S4F and S4G), implying that HRJD induction promotes turnover of midgut epithelial cells. Collectively, our data show that post-developmental expression of HRJDs improves stem cell functions in the aged intestine.

Discussion

In this study, we demonstrate that post-developmental expression of planarian HRJD genes in the *Drosophila* adult ISCs/EBs can suppress age-related intestinal dysfunctions and extend organismal lifespan, while their continuous expression throughout the entire developmental process hampers regenerative responses and principally shortens lifespan. Notably, HRJDs in adult ISCs/EBs boost the age-related increase of ISC proliferation but do not cause age-related mis-differentiation of ISC progenies (Fig. 7). These HRJD-mediated outcomes are distinct from those mediated by typical anti-aging manipulations such as antibiotic treatment and metabolic intervention, which ameliorate both ISC over-proliferation and mis-differentiation [24, 31, 49]. Therefore, heterologously induced HRJDs create the neomorphic state in the aged intestine (Fig. 7). Given the age-related increase of chronic cellular stresses [24, 27, 36, 49, 50], we speculate that the HRJD-dependent ISC activation and their proper differentiation improve organismal fitness by enabling active turnover of damaged intestinal cells.

Our investigation implies that the activation of the JAK-STAT pathway underlies the HRJD-mediated enhancement of ISC functions. Surprisingly, however, the expression of most mitogens including upstream ligands of JAK-STAT signaling (*upd1*, *upd2*, *upd3*) were not upregulated by HRJD induction (Additional file 1: Fig. S4H), raising the possibility that HRJDs activate STAT by modulating intracellular signaling factors. Such ligand-independent STAT activation can be achieved
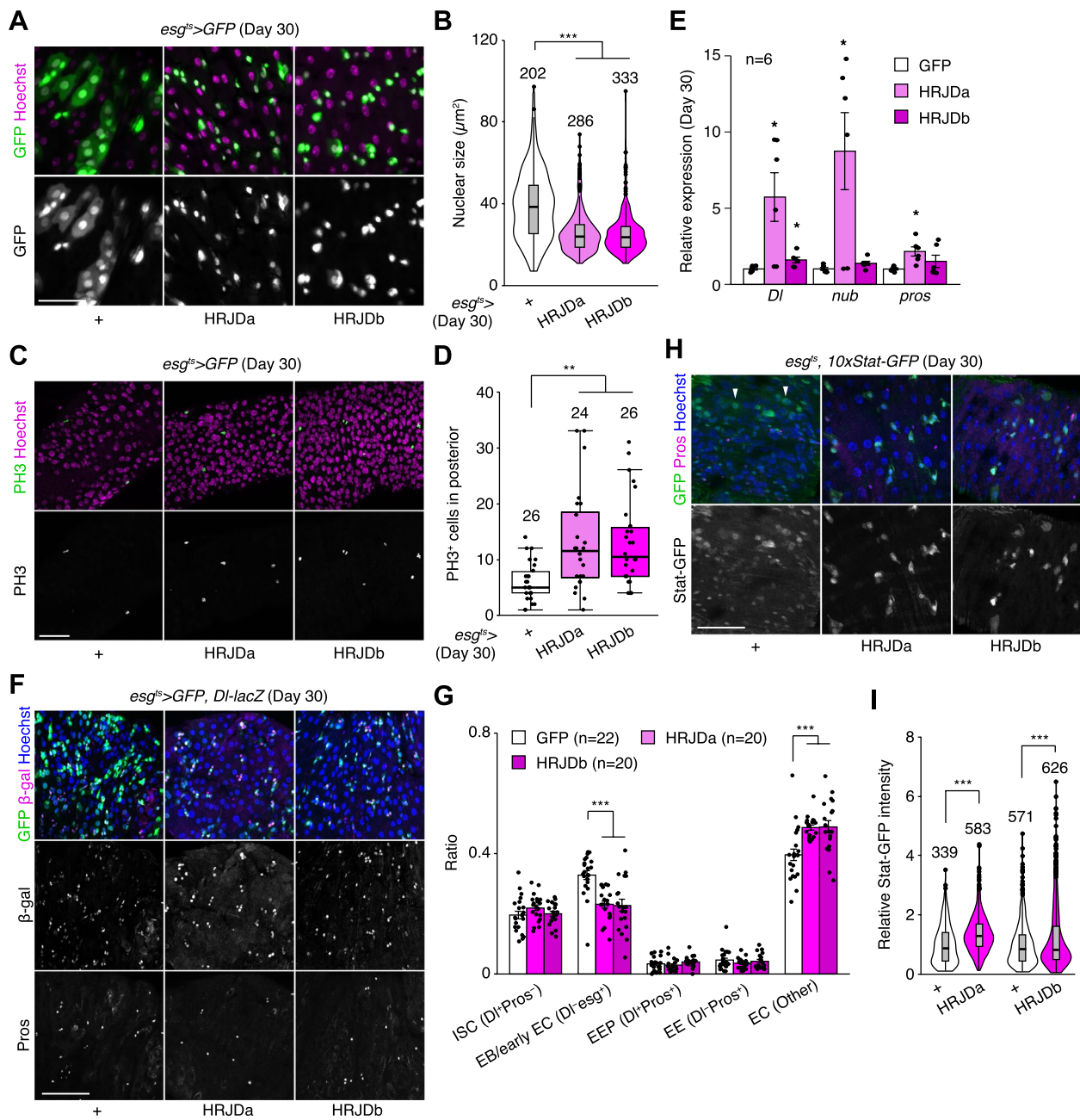
Nagai *et al. BMC Biology* (2024) 22:157

Page 10 of 16

Fig. 6 HRJD expression in adult ISCs/EBs improves stem cell functions in aged midguts. **A** Representative images for *esg-Gal4* positive cells in day 30 midguts. HRJDs suppressed mis-differentiation of *esg*+ cells (cellular enlargement with polyploid large nuclei). **B** Quantification of nuclear size of *esg-Gal4* positive cells. **C**, **D** Representative images (**C**) and quantification (**D**) of PH3 positive cells in day 30 posterior midguts. **E** RT-qPCR of *Dl*, *nub*, and *pros* in day 30 midguts. Expression levels were normalized to those of GFP control. **F**, **G** Cell type composition in aged midguts were assessed with *esg*ts *> GFP* (ISC, EB, and early EC), *Dl-lacZ* (ISC and EEP), and anti-Pros staining (EEP and EE). HRJD expression in adult ISCs/EBs reduced the ratio of EB/early EC and increased the ratio of EC (**G**). **H**, **I** *esg*ts-mediated HRJD induction enhanced STAT-GFP intensity in Pros⁻ diploid cells (ISCs/EBs), which is quantified in **I**. Additionally, HRJDs suppressed STAT activation in polyploid ECs (arrowheads). N.S., not significant: *P* > 0.05, **P* ≤ 0.05, ***P* ≤ 0.01, ****P* ≤ 0.001, one-way ANOVAs with post hoc Tukey test. *n* indicates the number of cells (**B**, **I**), guts (**D**, **G**), and biological replicates (**E**). Scale bars: 50 μm

via non-receptor type tyrosine kinases like Src and Abl [51]. Given that the typical JmjC family proteins function as histone demethylase or protein hydroxylase [52], HRJDs may epigenetically target these tyrosine kinases. Notably, *Drosophila* Jarid2 (Jumonji, AT rich interactive domain 2) activates EGFR signaling upon overexpression
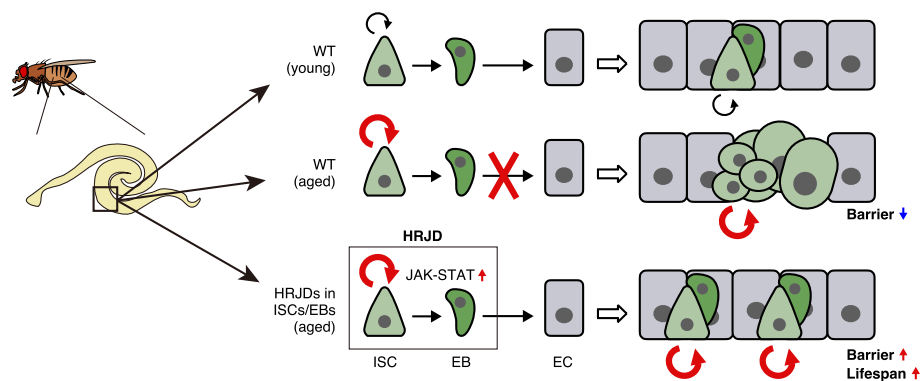
Nagai *et al. BMC Biology* (2024) 22:157

Page 11 of 16

Fig. 7 Graphical summary. Schematic model for the impact of HRJDs on intestinal homeostasis. In aged wildtype midguts, ISCs over-proliferate, and their daughters fail to differentiate into mature ECs, resulting in an accumulation of mis-differentiated cells (*esg*+ large polyploid). HRJD expression in adult ISCs/EBs further enhances ISC proliferation but suppresses mis-differentiation likely through upregulation of JAK-STAT signaling, which results in successful maintenance of the gut barrier and an extension of organismal lifespan

in ISCs/EBs without changing ligand expression [53]. Our findings, together with these reports, suggest a cell-autonomous role of JmjC family proteins in regulating proliferative signaling in stem cell lineages. Intriguingly, Jarid2 expression in ISCs/EBs leads to ISC over-proliferation as well as barrier dysfunction, resulting in reduced lifespan [53], which is the opposite adult phenotype of HRJD expression in ISC lineages. Moreover, in contrast to the nuclear localization of histone demethylase KDM8 [54, 55], the closest paralog of HRJDs, ectopically induced HRJDs localize in the cytoplasm but not in the nucleus both in vitro (S2 cells) and in vivo (wing discs and adult midguts) (Additional file 1: Fig. S1B-S1D). This is a common localization pattern of JmjC-domain only proteins [55, 56] and implies that an unknown mechanism may operate when HRJDs work as a potential histone demethylase. In the future, it will thus be critical to examine the detailed molecular function of HRJDs to understand their impact on stem cell lineages.

Although HRJDs have been identified as genes conserved between highly regenerative animals [13], it is unclear whether HRJDs alone are sufficient to enhance regenerative responses. Our investigations revealed that ectopic expression of HRJDs failed to improve regeneration of developing wing discs and adult midguts in *Drosophila* (Figs. 2 and 3), likely through the attenuation of regenerative growth. However, it should be noted that we induced HRJDs before tissue injury and maintained their expression during regeneration period. Given that *HRJDb* is upregulated in the late phase of planarian regeneration (3 days after amputation) [13], strict regulation of HRJD induction might be important for their proper function as true regeneration regulators. On the other hand, the expression level of *HRJDa* remains constant during planarian regeneration [13], which is recapitulated in our

experiments. Another possibility is that a high regeneration ability can be achieved by cooperation between HRJDs and other unidentified genes that have been lost during evolution, which should be addressed in future studies.

During the normal aging process in the *Drosophila* adult midgut, ISC over-proliferation is closely linked with other aging phenotypes, and suppression of ISC division can prevent the accumulation of mis-differentiated ISC progenies and extend organismal lifespan [24, 36, 49, 50]. In contrast, HRJDs enhance age-related ISC activation but can alleviate mis-differentiation and extend lifespan, suggesting that it is not ISC activation itself but rather mis-differentiation of ISC progenies that principally drives age-related mortality. Consistently, manipulation of mitotic spindle orientation, which affects the cell fate of daughter cells [57–59], can extend organismal lifespan without changing mitotic activity of ISCs [59]. Of note, in contrast to *Drosophila* ISCs which over-proliferate in aged midguts, many adult stem cells decrease their activity and abundance during aging both in *Drosophila* and mammals [24, 60, 61]. Future investigations for mechanisms of HRJD-mediated stem cell rejuvenation will provide clues to develop new anti-aging strategies.

Conclusions
In this study, we established a *Drosophila* model in which HRJDs are heterologously expressed in specific tissue or cell type using binary expression systems and demonstrated that HRJDs can improve proliferative/differentiation capacity of ISCs in the aged midgut. Although continuous HRJD expression in the wing disc and in the adult midgut impairs tissue regeneration upon injury, restricted HRJD expression in post-developmental adult ISCs/EBs enhances mitotic activity of ISCs as well as

Nagai *et al. BMC Biology* (2024) 22:157

Page 12 of 16

maintains their differentiation fidelity in the aged flies, leading to the prevention of age-related intestinal barrier dysfunction and the extension of organismal lifespan. Our HRJD-expressing model will serve as a valuable resource to understand unprecedented mechanisms of stem cell rejuvenation in the future.

Methods

Drosophila stocks

All stocks were maintained on a standard diet containing 4% cornmeal, 6% baker's yeast (Saf Yeast), 6% glucose (Wako, 049–31177), and 0.8% agar (Kishida chemical, 260–01705) with 0.3% propionic acid (Tokyo Chemical Industry, P0500) and 0.05% nipagin (Wako, 132–02635). Canton S was utilized as the wildtype strain. Transgenic fly lines were obtained from the Bloomington Drosophila Stock Center (BDSC, https://bdsc.indiana.edu/) and the Kyoto Stock Center (https://kyotofly.kit.jp/cgi-bin/stocks/index.cgi). Unless otherwise indicated, strain descriptions can be found at Flybase (http://flybase.bio.indiana.edu): *Act5C-Gal4* (BDSC 3954, described in Flybase and BDSC), *rn-Gal4*, *tub-Gal80ts*, *UAS-egr* [17] (BDSC 51280), *WP-QF2* [62], *tub-Gal80ts* (BDSC 7017, 7019, described in Flybase and BDSC), *esg-Gal4* [63] (Kyoto 109,126), *NP1-Gal4* [64] (Kyoto 112,001), *UAS-GFP* (BDSC 1521, described in Flybase and BDSC), *M{3xP3-RFP.attP}ZH-86Fb* [65] (Kyoto 130,437), *UAS-HRJDa* (this study), *UAS-HRJDb* (this study), *QUAS-HRJDa* (this study), *QUAS-HRJDb* (this study), *UAS-FLAG-HRJDa* (this study), *UAS-FLAG-HRJDb* (this study), *puc-lacZ* [66] (BDSC 98329), *10×STAT-GFP* [67] (BDSC 26198), *Dl-lacZ* [68] (BDSC 11651). *esg-Gal4, UAS-GFP, tub-Gal80ts; UAS-FLP, Act5C-FRT.CD2-Gal4* (esgFLPout) [26, 69] is a gift from Irene Miguel-Aliaga. See Additional file 2: Table S1 for genotypes in each figure. We used female flies unless otherwise noted in the figures.

Drosophila genetics

Experimental crosses that did not involve Gal80[ts]-mediated inhibition of Gal4 were performed at 25 ℃. When using Gal80[ts], experimental crosses were maintained at 18 ℃. For genetic wing ablation experiments (Fig. 2), F1 larvae were raised at 18 ℃ until day 7, incubated at 29 ℃ for the next 40 h, and then maintained at 18 ℃ until the adult hatched or dissection. For lifespan assays, midgut staining, and Smurf assays (Figs. 3, 4, 5, and 6), F1 adults were transferred to 29 ℃ 3 days after eclosion until the experiments. Midgut staining and Smurf assays were performed after 7 or 27 days of 29 ℃ incubation (young: day 10 adults, old: day 30 adults). For esgFLPout experiments, flies were maintained at 18 ℃

until 50 days, and 50-day old adults were transferred to 29 ℃ and analyzed after 10 days (final 60-day old).

Generation of HRJD expressing lines

To express HRJDs using the Gal4/UAS or the QF/QUAS system, we constructed a vector containing *HRJDa* or *HRJDb* under the control of either the UAS sequence or QUAS sequence. Namely, we amplified HRJDa and HRJDb sequence from codon-optimized synthesized DNAs (pUCIDT-HRJDa and pUCIDT-HRJDb, IDT, Additional file 3: Supplementary texts S1) for *DjHRJDa* (Genbank # LC408963) and *DjHRJDb* (Genbank # LC408964), respectively. UAS-HRJDa and UAS-HRJDb were constructed by ligating HRJDa and HRJDb into pUAST-attB (DGRC 1419), respectively (digested by EcoRI/NotI). Similarly, QUAS-HRJDa and QUAS-HRJDb were constructed by ligating HRJDa and HRJDb into pQUAS-WALIUM20 (DGRC 1474), respectively (digested by NheI/EcoRI). To construct UAS-3xFLAG-HRJDs, we PCR-amplified the coding sequences of HRJDs from pUCIDT-HRJDs by gene-specific primers with 3xFLAG tag at 5′-end of the forward primers, and the amplicons were then ligated into a pUAST-attB vector digested by EcoRI/NotI using In-Fusion HD Cloning Kit (Takara, 639,649). The landing site for each construct was {3xP3-RFP.attP}ZH-86Fb. Injection and selection were performed by WellGenetics (Taiwan, R.O.C.). Please see also Table S2 and Supplementary texts S1 for primer sequences and HRJDs sequences.

S2 cell culture

Drosophila S2 cells were grown at 25 ℃ in Schneider's *Drosophila* medium (GIBCO, 21,720,001) supplemented with 10% (v/v) heat-inactivated fetal bovine serum (FBS), 100 U/mL penicillin, and 100 μg/mL streptomycin (FUJIFILM Wako, 168–23,191).

S2 cell immunostaining

To examine the expression pattern of HRJDs through immunostaining, 1×10^6 cells were seeded in 6-well plates containing Schneider's *Drosophila* medium supplemented with 10% (v/v) heat-inactivated fetal bovine serum, 100 U/mL penicillin, and 100 μg/mL streptomycin and were transfected with 800 ng of pAc5-3xFLAG-HRJDs using Effectene Transfection Reagent (QIAGEN, 301,427) following the manufacturer's protocol. To prepare pAc5-3xFLAG-HRJDs, we amplified the coding sequences of HRJDs from pUCIDT-HRJDs (Additional file 3: Supplementary texts S1) by gene-specific primers with 3xFLAG tag at 5′-end of the forward primers, and the amplicons were then ligated into a pAc5-STABLE2-neo (Addgene, 32,426) [70] digested with EcoRI/XhoI by In-Fusion HD Cloning Kit (Takara, 639,649). Twenty-four

Nagai *et al. BMC Biology* (2024) 22:157

Page 13 of 16

hours after transfection, the cells were washed with PBS and the medium was replaced with fresh Schneider's *Drosophila* medium supplemented with 10% (v/v) heat-inactivated FBS, 100 U/mL penicillin, and 100 μg/mL streptomycin. Forty-eight hours after transfection, the cells were fixed with 4% paraformaldehyde (PFA) in PBS, washed with PBS containing 0.1% Triton X-100 (PBST), blocked in PBST with 5% normal donkey serum (PBSTn), and incubated with primary antibodies in PBSTn overnight at 4 °C. The samples were then washed with PBST, incubated for 1 h at room temperature with secondary antibodies and Hoechst 33,342 suspended in PBSTn and washed again with PBST. Images were captured using an LSM880 (Zeiss). The primary antibody used was a mouse anti-FLAG M2 monoclonal antibody (1:2000, Sigma, F1804). The secondary antibodies used were Goat anti-Mouse IgG2b Cross-Adsorbed Secondary Antibody, Alexa Fluor™ 555 (1:2000, Thermo Fisher Scientific, A-21147). Hoechst 33,342 (0.4 μM; Invitrogen, H3570) was used for nuclear staining. Images were analyzed and edited using Fiji/ImageJ software (NIH).

S2 cell western blotting

To examine the expression of HRJDs, 2.5×10^5 cells were seeded in 24-well plates containing Schneider's *Drosophila* medium supplemented with 10% (v/v) heat-inactivated FBS, 100 U/mL penicillin, and 100 μg/mL streptomycin and were transfected with 200 ng of pAc5-3xFLAG-HRJDs using Effectene Transfection Reagent (QIAGEN, 301,427) following the manufacturer's protocol. Twenty-four hours after transfection, the cells were washed with PBS, and the medium was replaced with fresh Schneider's *Drosophila* medium supplemented with 10% (v/v) heat-inactivated FBS, 100 U/mL penicillin, and 100 μg/mL streptomycin. Forty-eight hours after transfection, the cells were washed with PBS and lysed with 50 μL RIPA buffer supplemented with cOmplete ULTRA EDTA-free protease inhibitor cocktail (Roche, 05892953001). The lysate was sonicated and centrifuged at 20,000 g for 5 min. Protein concentration was determined by BCA assay. The supernatant was mixed with SDS, boiled at 95 °C for 5 min, and subjected to western blotting.

Proteins were separated using SDS-PAGE and transferred onto Immobilon-P PVDF membranes (Millipore, IPVH00010) for immunoblotting. Membranes were blocked with 4% skimmed milk diluted in $1 \times$ Tris buffered saline containing 0.1% Tween-20. Immunoblotting was performed using the below-mentioned antibodies, which were diluted with 4% skim milk. The signals were visualized using Immobilon Western Chemiluminescent HRP Substrate (Millipore, WBKLS0500) and FUSION SOLO. 7S. EDGE (Vilber-Lourmat). Contrast

and brightness adjustments were applied using the Fiji/ImageJ software (NIH).

The primary antibody used was mouse anti-FLAG M2 monoclonal antibody (1:5000, Sigma, F1804). Mouse anti-alpha tubulin (DM1A) monoclonal antibody (1:5000, Sigma, T9026) was used as loading control. The secondary antibody used was HRP-conjugated goat/rabbit/donkey anti-mouse IgG (1:10,000, Promega, W402B).

Drug treatment

5 mM paraquat (Sigma, 856,177) and 5% (w/v) DSS (MP Biomedicals, 160,110) were dissolved in 5% (w/v) sucrose solution. Filter paper (Whatman 3MM) was soaked with 400 μL of these reagents and placed into empty vials. For histological analyses, flies were fed with the reagent solution for 1 day. For the survival assay, flies were transferred to new vials and dead flies (determined by immobility and showing no response to tapping) were counted every day. 5% sucrose was used for control feeding.

Immunofluorescence

Samples were dissected in $1 \times$ PBS and fixed in 4% PFA for 20 min (wing discs) and 30–45 min (adult midgut) at room temperature (RT), respectively. The following primary antibodies were used with indicated dilution into $1 \times$ PBS containing 0.5% BSA and 0.1% Triton X-100: rabbit anti-PH3 (Millipore 06–570, 1:1000), mouse anti-FLAG (Sigma F1804, 1:1000), mouse anti-Dlg (DSHB 4F3, 1:100), rabbit anti-GFP (MBL 598, 1:500), rat anti-GFP (Nacalai tesque 04404–26, 1:400), rabbit anti-Tsp2A (Izumi et al., 2016, 1:1000) [71], rabbit anti-Mesh (Izumi et al., 2012, 1:1000) [72], rabbit anti-Ssk (Izumi et al., 2016, 1:1000) [71], chicken anti-β-galactosidase (Abcam ab9361, 1:500), anti-cDcp1 (Cell Signaling Technology 9578, 1:200). After overnight incubation with primary antibodies at 4 °C, samples were incubated with fluorescent secondary antibodies (Jackson ImmunoResearch and Invitrogen, 1:500) for 1 h at RT. Hoechst 33,342 (Invitrogen, final concentration: 10 μg/ml) was used to visualize DNA. Wing discs were mounted as described previously [73, 74]. Samples were mounted in Slowfade Diamond (ThermoFisher, S36963) and imaged with confocal microscopy Zeiss LSM880 or Zeiss LSM980.

Smurf assay

We referred to Rera et al. (2012) for the Smurf assay conditions [35]. To prepare the feeding medium, 100 μL of 50% (w/v) brilliant blue FCF (Wako, 027–12842, final 2.5%) and 100 μL of 5% (w/v) sucrose were added to a vial containing 2 ml of cornmeal-agar food. After mixing with a spatula, a Whatman 1 filter (1001–020) was put on the feeding medium. Flies were fed with this medium at 25 °C for 1 day, after which they were transferred to a new vial

Nagai *et al. BMC Biology* (2024) 22:157

Page 14 of 16

containing cornmeal-agar food without blue dye to clean the epidermis. Two hours after the transfer, Smurf phenotype was checked. We classified the Smurf phenotype as blue dye leakage outside abdomen (thorax, head, legs).

RT-qPCR
Total RNA was purified from 10 to 15 midguts using the ReliaPrep RNA Tissue Miniprep System (Promega). cDNA was made from 100 or 200 ng of RNA using PrimeScript RT Reagent Kit (TaKaRa). Quantitative PCR was performed using TB Green Premix Ex Taq II (TaKaRa) and the QuantStudio 6 Flex Real-Time PCR System (ThermoFisher). RpL32 was used as an internal control. Primer sequences are listed in Additional file 4: Table S2.

Phylogenetic tree
We created the phylogenetic tree of representative organisms using the NCBI taxonomy browser (https://www.ncbi.nlm.nih.gov/Taxonomy/CommonTree/wwwcmt.cgi). The species examined are *Amphimedon queenslandica* (Porifera), *Mnemiopsis leidyi* (Ctenophora), *Trichoplax adhaerens* (Placozoa), *Hydra vulgaris* (Cnidaria), *Ptychodera flava* (Hemichordata), *Acanthaster planci* (Echinodermata), *Branchiostoma floridae* (Cephalochordata), *Ciona intestinalis* (Tunicata), *Danio rerio* (Teleostei), *Homo sapiens*, *Mus musculus* (Mammalia), *Schmidtea mediterranea* (Platyhelminthes), *Caenorhabditis elegans* (Nematoda), and *Drosophila melanogaster* (Arthropoda). These species, except for *D. rerio*, *H. sapiens*, *M. musculus*, *C. elegans*, and *D. melanogaster*, are known to have HRJDs and exhibit high regeneration ability [13]. The pictures were downloaded from PhyloPic, and the color of some were changed from black to blue. Credits: Bennet McComish (*B. floridae*), Malio Kodis (*M. leidyi*), and Markus A. Grohme (*S. mediterranea*, https://www.phylopic.org/images/93f9611c-0cbd-4a14-92da-004a4521e21f/schmidtea-mediterranea).

Quantification of PH3 positive cells
For wing discs, we counted PH3 positive cells in the pouch region, which develops into the adult wing. After binarization, the number of PH3 positive cells was counted using the Analyze Particles function in Fiji/ImageJ and subsequently confirmed or corrected by visual review of the images. For adult midguts, the number of PH3 positive cells in the posterior midguts was manually counted.

Quantification of junctional proteins
To quantify junctional and cytoplasmic intensity, a line that was orthogonal to one side of a cell was drawn, and then the plot profile was calculated for the line. We defined the junctional intensity as the highest value in that profile and defined cytoplasmic intensity as the value 20 pixels (~ 2.6 μm) away from the highest value. Three lines were drawn for one cell and the average of the three was used to represent the junctional/cytoplasmic ratio for the cell. Six polyploid cells were randomly selected from each image for quantification.

Quantification of reporter intensity
The signal intensity of *puc-lacZ* and *10×STAT-GFP* reporters was quantified using Fiji/ImageJ. The nuclei of large polyploid cells (for *puc-lacZ*) and Pros⁻ diploid cells (for *10×STAT-GFP*) were selected as ROIs using the polygon selection tool. The reporter intensity in each ROI was quantified using the Measure command.

Quantification of nuclear size
Nuclei of *esg-Gal4 > UAS-GFP* positive cells were traced by the polygon selection tool and added as ROI in Fiji/ImageJ. The size of each ROI was quantified using the Measure command.

Quantification of cell number
Cell number was quantified using Fiji/ImageJ. To count the total cell number, Hoechst signal was processed as following: (1) despeckle, (2) binarization, (3) fill hole, (4) watershed, (5) analyze particle. The following cell number was manually counted using the cell counter function: *esg > GFP*⁺ cells, *Dl-lacZ*⁺ cells, Pros⁺ cells, and cDcp1⁺ cells.

Statistics
Statistical analyses were performed using Excel and RStudio. Two tailed *t* tests were used for comparisons between two groups. One-way ANOVAs with post hoc Tukey tests were performed when comparing three or more groups. Log-rank tests were used for comparison of survival curve. Significance is indicated in the figures as follows: $^*P \leq 0.05$, $^{**}P \leq 0.01$, $^{***}P \leq 0.001$, not significant (N.S.): $P > 0.05$. Bar graphs show mean ± standard error. Boxplots show median (thick line in the box), first and third quartiles (bottom and top of the box), minimum value (lower whisker), and maximum value (upper whisker). Dots in bar graphs and boxplots indicate individual values. Violin plots portray the distribution of individual values.

Abbreviations
i-cell	interstitial cell
HRJD	Highly regenerative species-specific JmjC domain-encoding gene
PH3	Phospho-histone H3
ISC	Intestinal stem cell
EB	Enteroblast
EEP	Enteroendocrine progenitor
EC	Enterocyte
EE	Enteroendocrine cell
DSS	Dextran sulfate sodium

Nagai *et al. BMC Biology* (2024) 22:157

Page 15 of 16

puc   Puckered
Dl   Delta
Jarid2   Jumonji, AT rich interactive domain 2

Supplementary Information

The online version contains supplementary material available at https://doi.org/10.1186/s12915-024-01956-4.

Additional file 1: Figs. S1-S4. Fig. S1 - Expression and localization of HRJD proteins. Fig. S2 - Continuous expression of HRJDs throughout development hampers intestinal regeneration. Fig. S3 - Organismal lifespan of flies expressing HRJDs in ECs and ISC/EBs. Fig. S4 - HRJD induction in adult ISCs/EBs promotes turnover of midgut epithelial cells.

Additional file 2: Table S1. Detailed genotypes in each experiment.

Additional file 3: Supplementary texts S1. Sequences for pUCIDT-HRJDa and pUCIDT-HRJDb.

Additional file 4: Table S2. Primer sequences.

Authors' contributions

HN and YN conceived and designed the study; HN, YA, TN, ET, JU, and YN conducted experiments and validated results; TM prepared the experimental material; HN, JU, TM, and YN wrote the original draft; HN, JU, and YN designed the figures; HN and YN revised the manuscript; YN and MM supervised the study. All authors read and approved the manuscript.

Availability of data and materials

All data generated or analyzed during this study are included in this published article and its supplementary information files. *Drosophila* stocks used and/or analyzed during the current study are available from the corresponding author on reasonable request.

Declarations

Ethics approval and consent to participate

Not applicable.

Consent for publication

Not applicable.

Competing interests

The authors declare that they have no competing interests.

References

1. Bely AE, Nyberg KG. Evolution of animal regeneration: re-emergence of a field. Trends Ecol Evol. 2010;25:161–70.
2. Poss KD. Advances in understanding tissue regenerative capacity and mechanisms in animals. Nat Rev Genet. 2010;11:710–22.
3. Tiozzo S, Copley RR. Reconsidering regeneration in metazoans: an evo-devo approach. Front Ecol Evol. 2015;3:67.
4. Bideau L, Kerner P, Hui J, Vervoort M, Gazave E. Animal regeneration in the era of transcriptomics. Cell Mol Life Sci. 2021;78:3941–56.
5. Fujita S, Kuranaga E, Nakajima Y. Regeneration potential of jellyfish: cellular mechanisms and molecular insights. Genes. 2021;12:758.
6. Piraino S, Boero F, Aeschbach B, Schmid V. Reversing the life cycle: medusae transforming into polyps and cell transdifferentiation in *Turritopsis nutricula* (Cnidaria, Hydrozoa). Biol Bull. 1996;190:302–12.
7. Varley Á, Horkan HR, McMahon ET, Krasovec G, Frank U. Pluripotent, germ cell competent adult stem cells underlie cnidarian regenerative ability and clonal growth. Curr Biol. 2023;33:1883–1892.e3.
8. Gazave E, Röttinger E. 7th Euro Evo Devo meeting: Report on the "Evolution of regeneration in Metazoa" symposium. J Exp Zoolog B Mol Dev Evol. 2021;336:89–93.
9. Kumar A, Godwin JW, Gates PB, Garza-Garcia AA, Brockes JP. Molecular basis for the nerve dependence of limb regeneration in an adult vertebrate. Science. 2007;318:772–7.
10. Da Silva SM, Gates PB, Brockes JP. The newt ortholog of CD59 is implicated in proximodistal identity during amphibian limb regeneration. Dev Cell. 2002;3:547–55.
11. Looso M, Preussner J, Sousounis K, Bruckskotten M, Michel CS, Lignelli E, et al. A de novo assembly of the newt transcriptome combined with proteomic validation identifies new protein families expressed during tissue regeneration. Genome Biol. 2013;14:R16.
12. Mehta AS, Deshpande P, Chimata AV, Tsonis PA, Singh A. Newt regeneration genes regulate Wingless signaling to restore patterning in Drosophila eye. iScience. 2021;24:103166.
13. Cao P-L, Kumagai N, Inoue T, Agata K, Makino T. JmjC domain-encoding genes are conserved in highly regenerative metazoans and are associated with planarian whole-body regeneration. Genome Biol Evol. 2019;11:552–64.
14. Umesono Y, Tasaki J, Nishimura Y, Hrouda M, Kawaguchi E, Yazawa S, et al. The molecular logic for planarian regeneration along the anterior–posterior axis. Nature. 2013;500:73–6.
15. Brand AH, Perrimon N. Targeted gene expression as a means of altering cell fates and generating dominant phenotypes. Development. 1993;118:401–15.
16. Hariharan IK, Serras F. Imaginal disc regeneration takes flight. Curr Opin Cell Biol. 2017;48:10–6.
17. Smith-Bolton RK, Worley MI, Kanda H, Hariharan IK. Regenerative growth in Drosophila imaginal discs is regulated by Wingless and Myc. Dev Cell. 2009;16:797–809.
18. Worley MI, Alexander LA, Hariharan IK. CtBP impedes JNK- and Upd/STAT-driven cell fate misspecifications in regenerating Drosophila imaginal discs. eLife. 2018;7:e30391.
19. Potter CJ, Tasic B, Russler EV, Liang L, Luo L. The Q system: a repressible binary system for transgene expression, lineage tracing, and mosaic analysis. Cell. 2010;141:536–48.
20. Riabinina O, Luginbuhl D, Marr E, Liu S, Wu MN, Luo L, et al. Improved and expanded Q-system reagents for genetic manipulations. Nat Methods. 2015;12:219–22.
21. Nagai H, Miura M, Nakajima Y. Cellular mechanisms underlying adult tissue plasticity in Drosophila. Fly (Austin). 2022;16:190–206.
22. Miguel-Aliaga I, Jasper H, Lemaitre B. Anatomy and physiology of the digestive tract of *Drosophila melanogaster*. Genetics. 2018;210:357–96.
23. Zhang P, Edgar BA. Insect gut regeneration. Cold Spring Harb Perspect Biol. 2021;:a040915.
24. Jasper H. Intestinal stem cell aging: origins and interventions. Annu Rev Physiol. 2020;82:203–26.
25. Buchon N, Broderick NA, Chakrabarti S, Lemaitre B. Invasive and indigenous microbiota impact intestinal stem cell activity through multiple pathways in *Drosophila*. Genes Dev. 2009;23:2333–44.
26. Jiang H, Patel PH, Kohlmaier A, Grenley MO, McEwen DG, Edgar BA. Cytokine/Jak/Stat signaling mediates regeneration and homeostasis in the Drosophila midgut. Cell. 2009;137:1343–55.
27. Biteau B, Hochmuth CE, Jasper H. JNK activity in somatic stem cells causes loss of tissue homeostasis in the aging Drosophila gut. Cell Stem Cell. 2008;3:442–55.
28. Amcheslavsky A, Jiang J, Ip YT. Tissue damage-induced intestinal stem cell division in Drosophila. Cell Stem Cell. 2009;4:49–61.
29. Jiang H, Edgar BA. EGFR signaling regulates the proliferation of *Drosophila* adult midgut progenitors. Development. 2009;136:483–93.

Nagai *et al. BMC Biology* (2024) 22:157

Page 16 of 16

30. Houtz P, Bonfini A, Bing X, Buchon N. Recruitment of adult precursor cells underlies limited repair of the infected larval midgut in Drosophila. Cell Host Microbe. 2019;26:412–425.e5.

31. Rera M, Bahadorani S, Cho J, Koehler CL, Ulgherait M, Hur JH, et al. Modulation of longevity and tissue homeostasis by the Drosophila PGC-1 homolog. Cell Metab. 2011;14:623–34.

32. Thevaranjan N, Puchta A, Schulz C, Naidoo A, Szamosi JC, Verschoor CP, et al. Age-associated microbial dysbiosis promotes intestinal permeability, systemic inflammation, and macrophage dysfunction. Cell Host Microbe. 2017;21:455–466.e4.

33. Nagai H, Tatara H, Tanaka-Furuhashi K, Kurata S, Yano T. Homeostatic regulation of ROS-triggered Hippo-Yki pathway via autophagic clearance of Ref(2)P/p62 in the Drosophila intestine. Dev Cell. 2021;56:81–94.e10.

34. Egge N, Arneaud SLB, Wales P, Mihelakis M, McClendon J, Fonseca RS, et al. Age-onset phosphorylation of a minor actin variant promotes intestinal barrier dysfunction. Dev Cell. 2019;51:587–601.e7.

35. Rera M, Clark RI, Walker DW. Intestinal barrier dysfunction links metabolic and inflammatory markers of aging to death in Drosophila. Proc Natl Acad Sci. 2012;109:21528–33.

36. Resnik-Docampo M, Koehler CL, Clark RI, Schinaman JM, Sauer V, Wong DM, et al. Tricellular junctions regulate intestinal stem cell behaviour to maintain homeostasis. Nat Cell Biol. 2017;19:52–9.

37. Salazar AM, Resnik-Docampo M, Ulgherait M, Clark RI, Shirasu-Hiza M, Jones DL, et al. Intestinal snakeskin limits microbial dysbiosis during aging and promotes longevity. iScience. 2018;9:229–43.

38. Izumi Y, Furuse K, Furuse M. Septate junctions regulate gut homeostasis through regulation of stem cell proliferation and enterocyte behavior in *Drosophila*. J Cell Sci. 2019;:jcs.232108.

39. Chen H, Zheng X, Zheng Y. Age-associated loss of lamin-B leads to systemic inflammation and gut hyperplasia. Cell. 2014;159:829–43.

40. Korzelius J, Naumann SK, Loza-Coll MA, Chan JS, Dutta D, Oberheim J, et al. *Escargot* maintains stemness and suppresses differentiation in *Drosophila* intestinal stem cells. EMBO J. 2014;33:2967–82.

41. Li Y, Pang Z, Huang H, Wang C, Cai T, Xi R. Transcription factor antagonism controls enteroendocrine cell specification from intestinal stem cells. Sci Rep. 2017;7:988.

42. Zhou F, Rasmussen A, Lee S, Agaisse H. The UPD3 cytokine couples environmental challenge and intestinal stem cell division through modulation of JAK/STAT signaling in the stem cell microenvironment. Dev Biol. 2013;373:383–93.

43. Zhai Z, Boquete J-P, Lemaitre B. A genetic framework controlling the differentiation of intestinal stem cells during regeneration in Drosophila. PLOS Genet. 2017;13: e1006854.

44. Hudry B, De Goeij E, Mineo A, Gaspar P, Hadjieconomou D, Studd C, et al. Sex differences in intestinal carbohydrate metabolism promote food intake and sperm maturation. Cell. 2019;178:901–918.e16.

45. Liang J, Balachandra S, Ngo S, O'Brien LE. Feedback regulation of steady-state epithelial turnover and organ size. Nature. 2017;548:588–91.

46. Antonello ZA, Reiff T, Ballesta-Illan E, Dominguez M. Robust intestinal homeostasis relies on cellular plasticity in enteroblasts mediated by miR-8-Escargot switch. EMBO J. 2015;34:2025–41.

47. Xing Y, Su TT, Ruohola-Baker H. Tie-mediated signal from apoptotic cells protects stem cells in Drosophila melanogaster. Nat Commun. 2015;6:7058.

48. Jin Z, Chen J, Huang H, Wang J, Lv J, Yu M, et al. The Drosophila ortholog of mammalian transcription factor Sox9 regulates intestinal homeostasis and regeneration at an appropriate level. Cell Rep. 2020;31: 107683.

49. Clark RI, Salazar A, Yamada R, Fitz-Gibbon S, Morselli M, Alcaraz J, et al. Distinct shifts in microbiota composition during Drosophila aging impair intestinal function and drive mortality. Cell Rep. 2015;12:1656–67.

50. Wang L, Ryoo HD, Qi Y, Jasper H. PERK limits Drosophila lifespan by promoting intestinal stem cell proliferation in response to ER stress. PLOS Genet. 2015;11: e1005220.

51. Hu X, Li J, Fu M, Zhao X, Wang W. The JAK/STAT signaling pathway: from bench to clinic. Signal Transduct Target Ther. 2021;6:402.

52. Markolovic S, Leissing TM, Chowdhury R, Wilkins SE, Lu X, Schofield CJ. Structure–function relationships of human JmjC oxygenases—demethylases versus hydroxylases. Curr Opin Struct Biol. 2016;41:62–72.

53. Suong DNA, Shimaji K, Pyo J-H, Park J-S, Yoshida H, Yoo M-A, et al. Overexpression of dJmj differentially affects intestinal stem cells and differentiated enterocytes. Cell Signal. 2018;42:194–210.

54. Hsia DA, Tepper CG, Pochampalli MR, Hsia EYC, Izumiya C, Huerta SB, et al. KDM8, a H3K36me2 histone demethylase that acts in the cyclin A1 coding region to regulate cancer cell proliferation. Proc Natl Acad Sci. 2010;107:9671–6.

55. Shalaby NA, Sayed R, Zhang Q, Scoggin S, Eliazer S, Rothenfluh A, et al. Systematic discovery of genetic modulation by Jumonji histone demethylases in Drosophila. Sci Rep. 2017;7:5240.

56. Klose RJ, Kallin EM, Zhang Y. JmjC-domain-containing proteins and histone demethylation. Nat Rev Genet. 2006;7:715–27.

57. Nakajima Y. Mitotic spindle orientation in epithelial homeostasis and plasticity. J Biochem (Tokyo). 2018;164:277–84.

58. Goulas S, Conder R, Knoblich JA. The Par complex and integrins direct asymmetric cell division in adult intestinal stem cells. Cell Stem Cell. 2012;11:529–40.

59. Hu DJ-K, Jasper H. Control of intestinal cell fate by dynamic mitotic spindle repositioning influences epithelial homeostasis and longevity. Cell Rep. 2019;28:2807–23 e5.

60. Brunet A, Goodell MA, Rando TA. Ageing and rejuvenation of tissue stem cells and their niches. Nat Rev Mol Cell Biol. 2023;24:45–62.

61. Campisi J, Kapahi P, Lithgow GJ, Melov S, Newman JC, Verdin E. From discoveries in ageing research to therapeutics for healthy ageing. Nature. 2019;571:183–92.

62. Kashio S, Obata F, Zhang L, Katsuyama T, Chihara T, Miura M. Tissue nonautonomous effects of fat body methionine metabolism on imaginal disc repair in *Drosophila*. Proc Natl Acad Sci. 2016;113:1835–40.

63. Goto S, Hayashi S. Proximal to distal cell communication in the Drosophila leg provides a basis for an intercalary mechanism of limb patterning. Development. 1999;126:3407–13.

64. Hayashi S, Ito K, Sado Y, Taniguchi M, Akimoto A, Takeuchi H, et al. GETDB, a database compiling expression patterns and molecular locations of a collection of gal4 enhancer traps. Genesis. 2002;34:58–61.

65. Bischof J, Maeda RK, Hediger M, Karch F, Basler K. An optimized transgenesis system for Drosophila using germ-line-specific φC31 integrases. Proc Natl Acad Sci. 2007;104:3312–7.

66. Martin-Blanco E, Gampel A, Ring J, Virdee K, Kirov N, Tolkovsky AM, et al. puckered encodes a phosphatase that mediates a feedback loop regulating JNK activity during dorsal closure in Drosophila. Genes Dev. 1998;12:557–70.

67. Bach EA, Ekas LA, Ayala-Camargo A, Flaherty MS, Lee H, Perrimon N, et al. GFP reporters detect the activation of the Drosophila JAK/STAT pathway in vivo. Gene Expr Patterns. 2007;7:323–31.

68. Röttgen G, Wagner T, Hinz U. A genetic screen for elements of the network that regulates neurogenesis in Drosophila. Mol Gen Genet MGG. 1998;257:442–51.

69. Hudry B, Khadayate S, Miguel-Aliaga I. The sexual identity of adult intestinal stem cells controls organ size and plasticity. Nature. 2016;530:344–8.

70. González M, Martín-Ruíz I, Jiménez S, Pirone L, Barrio R, Sutherland JD. Generation of stable Drosophila cell lines using multicistronic vectors. Sci Rep. 2011;1:75.

71. Izumi Y, Motoishi M, Furuse K, Furuse M. A tetraspanin regulates septate junction formation in *Drosophila* midgut. J Cell Sci. 2016;:jcs.180448.

72. Izumi Y, Yanagihashi Y, Furuse M. A novel protein complex, mesh-ssk, is required for septate junction formation in *drosophila* midgut. J Cell Sci. 2012;:jcs.112243.

73. Nakajima Y. Analysis of epithelial architecture and planar spindle orientation in the Drosophila wing disc. In: Turksen K, editor. Stem Cell Renewal and Cell-Cell Communication. Methods Mol Biol. 2021;2346:51–62.

74. Nakajima Y, Lee ZT, McKinney SA, Swanson SK, Florens L, Gibson MC. Junctional tumor suppressors interact with 14-3-3 proteins to control planar spindle alignment. J Cell Biol. 2019;218:1824–38.

Publisher's Note